DcaP-Family Porins are Required for Carboxylic Acid Catabolism in *Acinetobacter baumannii*

Hannah R. Noel[1], Jonathan D. Winkelman[2], Lauren D. Palmer[1]*

[1] Department of Microbiology and Immunology, University of Illinois Chicago, Chicago, IL, USA

[2] Trestle LLC, Milwaukee, WI, USA

*Corresponding author

Lauren D. Palmer

835 S Wolcott Ave

MSB E703

Chicago, IL 60612

ldpalmer@uic.edu

ABSTRACT

Acinetobacter baumannii is a pathogen of concern and a leading cause of multidrug-resistant healthcare-associated infections. The *A. baumannii* outer membrane is a barrier to antimicrobials and host defenses but must also allow essential nutrients to permeate. Here, we investigate the functional importance of the putative DcaP-family outer membrane porins, which include a proposed vaccine target in *A. baumannii*. All *A. baumannii* genomes surveyed encode multiple DcaP family porins, which we classify in four classes based on protein sequence phylogeny (DcaP1-4). DcaP proteins encoded by species in other genera could not be mapped to these DcaP classes and phylogenetic analysis suggests DcaP1-4 proteins diversified within *Acinetobacter*. Phenotypic array assays and additional experiments show that DcaP3 was necessary for growth on multiple di- and tri-carboxylic acids as sole carbon sources, including citric acid and tricarballylic acid. Finally, a mutant lacking all DcaP proteins was attenuated in the liver and spleen in a mouse model of bloodstream infection and complemented by expression of DcaP3. These findings provide insight on how *A. baumannii* acquires nutrients through the outer membrane barrier and show DcaP3 is important during infection in specific host niches, validating its potential as a therapeutic target.

30 **INTRODUCTION**

31 *Acinetobacter baumannii* is a pathogen of critical concern and a major cause of
32 healthcare-associated infections. Isolates of *A. baumannii* are often multidrug resistant (MDR)
33 or extensively drug resistant (XDR) and exhibit resistance to first and last line antibiotics, such
34 as meropenem and colistin, respectively (1). The Centers for Disease Control and the World
35 Health Organization have therefore identified *A. baumannii* as an urgent public health threat,
36 calling for new avenues of treatment (2–4). The bacterial cell envelope is the primary barrier
37 from the environment and protects bacteria from environmental stress including antibiotics and
38 host defenses; however, the cell envelope must also allow acquisition of essential nutrients and
39 cofactors (5,6). The outer membrane (OM) of *A. baumannii* is thought to be less permeable
40 compared to other Gram-negative bacteria such as *E. coli*, contributing to intrinsic antibiotic
41 resistance (7). How small molecule nutrients required for growth transit the impermeable OM in
42 *A. baumannii* is incompletely understood.

43 The OM of *A. baumannii* is an asymmetric lipid bilayer where the inner leaflet is
44 composed of glycerophospholipids and the outer leaflet of lipooligosaccharides (LOS) (5,8,9).
45 The OM bilayer is occupied by proteins that serve a variety of functions, including nutrient influx.
46 Nutrients typically pass through the OM via active transport by TonB-dependent transporters or
47 passive diffusion through porins which are transmembrane channels that allow passage of small
48 molecules (6,10). The primary porin in *A. baumannii* is OmpA, which shows slow molecular
49 transport in liposome swelling assays, contributing to the low permeability barrier of the OM (11–
50 13). However, the primary function of OmpA is thought to be structural, providing a physical
51 tether between the OM and the peptidoglycan cell wall in *A. baumannii* and other species
52 (14,15). *A. baumannii* encodes multiple other porins including CarO, an OM porin that
53 selectively allows influx of ornithine and other basic amino acids (16), and the Occ family porins,
54 responsible for the influx of compounds like benzoate, hydroxycinnamate, and other aromatic
55 molecules (17–19). The protein DcaP is a predicted OM porin widely distributed across

56 *Acinetobacter* species named for its localization within a genetic locus for utilization of
57 dicarboxylic acids (*dca*) (20). Notably, a DcaP family protein is among the most abundant OM
58 proteins in *A. baumannii* during rat and mouse infections (21). Due to this fact, multiple groups
59 have studied a DcaP-like protein as a promising vaccine candidate for protection against *A.*
60 *baumannii* infection (21–25). However, the biological role of DcaP family proteins remains
61 unclear.

62 First identified in Parke *et al*. as part of the dicarboxylic acid catabolic operon of
63 *Acinetobacter baylyi* ADP1, *dcaP* (dicarboxylic acid porin) and DcaP-like proteins were thought
64 to be specific to the Moraxellaceae family (20). The structure for one DcaP family protein has
65 been solved, presenting as a homo-trimeric 16-stranded beta-barrel protein with an extended
66 periplasmic N-terminus that forms a coiled coil (21). Due to the genetic localization and
67 induction of expression with the dicarboxylic acid adipate, *A. baylyi* DcaP-like proteins were
68 proposed to be nonspecific porins that facilitate the uptake of dicarboxylic acids (20); however, a
69 role for DcaP-like proteins in carboxylic acid catabolism has not been reported. Molecular
70 dynamics and electrophysiology studies determined a DcaP-like protein to have an affinity for
71 anionic compounds as substrates, such as the clinically relevant β-lactamase inhibitor
72 sulbactam (21). In other studies, DcaP-like proteins have been implicated in biofilm formation
73 and mucin catabolism (26,27). Here, we describe four classes of DcaP-like proteins in
74 *Acinetobacter* and investigate their role in carbon source utilization.
75

76 **RESULTS**

77 *Acinetobacter spp. encode multiple DcaP-family porins*

78 The first DcaP was described in *A. baylyi* as part of a dicarboxylic acid catabolic operon
79 (20), and DcaP-like proteins have been identified in various *A. baumannii* clinical isolates and
80 type-strains (21,23). Proteins designated DcaP-like in *A. baumannii* ATCC 17978 are
81 homologous to *A. baylyi* DcaP, sharing ~30-35% amino acid identity by Clustal Omega multiple

82 sequence alignment (28). However, given the abundance of DcaP-like proteins within individual
83 *Acinetobacter* genomes, we hypothesized that these proteins could be further classified based
84 on protein sequence. Using DcaP and DcaP-like sequences from a set of deduplicated *A.*
85 *baumannii* genomes, four distinct classes of DcaP-like proteins were identified that cluster
86 independently, including the original DcaP which we display as DcaP1 (Fig. 1A, S1A). We next
87 determined the distribution of DcaP-like proteins across the *Acinetobacter* genus. Using a set of
88 250 deduplicated *Acinetobacter* genomes, most of which were *A. baumannii*, DcaP proteins
89 were shown to be widely conserved across the genus (Fig. S1B). Additionally, *Acinetobacter*
90 species within the *A. calcoaceticus/baumannii* (*acb*) complex/clade of pathogenic *Acinetobacter*
91 appeared to be enriched for having multiple DcaP proteins compared to non-pathogenic
92 *Acinetobacter* species (Fig. S1B). Among the *A. baumannii* genomes, over 130 of the strains
93 encode four *dcaP* genes (Fig. 1B). In fact, no *A. baumannii* genome analyzed encoded fewer
94 than two *dcaP* genes (Fig. 1B). To determine if the *dcaP* genes were equally distributed across
95 the species, the number of each DcaP subfamily were tallied for each genome and organized
96 based on how many total DcaP proteins were present. The four classes of DcaP proteins were
97 equally likely to be encoded in a given *A. baumannii* genome (Fig. 1B). For example, in most
98 cases where a genome encodes four DcaP proteins, it was most likely to have one of each
99 variant. Alternatively, in a genome encoding five DcaP proteins, DcaP2 was most likely to be
100 duplicated. These data suggest that DcaP proteins are encoded across the *Acinetobacter*
101 genus, and enriched in pathogenic *Acinetobacter,* including *A. baumannii*.
102
103 *DcaP proteins from other bacterial species are distinct from Acinetobacter DcaP proteins*
104 To investigate the evolutionary history of DcaP proteins in *Acinetobacter* and determine if
105 DcaP diversified within *Acinetobacter* or across phyla, orthologues in other bacterial phyla were
106 identified through KEGG. Bacterial phyla were selected for further analysis if the DcaP-like
107 protein was encoded in more than half of the genomes for a given genus (29,30). A rooted

108 phylogenomic tree was generated to demonstrate the evolutionary distance between
109 *Acinetobacter* and the bacteria containing a DcaP orthologue (Fig. 2A). Orthologues of DcaP
110 proteins were found in distantly related organisms, such as *Shewanella spp.* and *Xanthomonas*
111 *spp.,* albeit generally in fewer numbers (Fig. 2A). These DcaP orthologues could not be further
112 classified into one of the four DcaP classes defined in *A. baumannii*. This suggests that the four
113 DcaP classes of proteins defined here are unique to *Acinetobacter spp*. To better understand
114 the relationship between *Acinetobacter* DcaP proteins and proteins designated DcaP-like from
115 distantly related species, an unrooted tree of protein sequences was generated. This analysis
116 revealed that DcaP proteins from AB5075, the included reference *A. baumannii* strain which
117 encodes DcaP1-4, were more similar to each other than to non-*Acinetobacter* DcaP proteins
118 (Fig. 2B). This suggests that diversification of the four DcaP classes defined here occurred
119 within *Acinetobacter*. In contrast to *A. baumannii*, multiple DcaP-like proteins encoded in other
120 organisms were sequence divergent, such as in *Pseudoxanthomonas daejeonensis*,
121 *Stenotrophomonas spp*., *Shewanella psychrotolerans*, and *Marinobacter spp.* (Fig 2B).
122 Comparison of the species phylogeny and DcaP protein phylogeny suggest there may have
123 been occurrences of horizontal gene transfer in other species outside *Acinetobacter*. Overall,
124 these data suggest that DcaP-like proteins are encoded by species across Proteobacteria and
125 that DcaP diversification has occurred within the *Acinetobacter* clade.
126
127 *DcaP family porins are necessary for growth on select di- and tri-carboxylic acids*
128 Next, we hypothesized that the DcaP-family porins are involved in small molecule
129 uptake. One study suggested that DcaP3 may translocate the clinically relevant beta-lactamase
130 inhibitor sulbactam based on electrophysiology and applied field simulation data (21).
131 Sulbactam is a therapeutic often used in combination with beta-lactam antibiotics like ampicillin
132 for bacteria with beta-lactam resistance. Many *A. baumannii* isolates are intrinsically resistant to
133 ampicillin due to the expression of beta-lactamases and sulbactam has been shown to

134 resensitize resistant isolates to beta-lactam antibiotics (31,32). We reasoned that if DcaP
135 proteins facilitated sulbactam entry, a ΔΔΔ*dcaP* mutant would exclude sulbactam from entering
136 the cell and result increased resistance to the beta-lactam ampicillin while a wild-type strain
137 would exhibit a re-sensitization to ampicillin. However, the wild-type and the ΔΔΔ*dcaP* mutant
138 strains exhibited similar sensitivities to ampicillin/sulbactam treatment (Fig. S2). These data
139 suggest that DcaP proteins are not required for sulbactam activity.
140 We next hypothesized that DcaP porins may be important for growth on certain nutrient
141 sources such as dicarboxylic acids as previously suggested (20). The growth of wild-type and
142 ΔΔΔ*dcaP* strains were compared using the high-throughput Biolog PM system to screen for
143 carbon source usage. Multiple compounds were identified on which wildtype was able to grow
144 but ΔΔΔ*dcaP* had a defect, and compounds where ΔΔΔ*dcaP* grew more than wildtype (Fig. 3A-
145 B). Many of the compounds in which WT grew better than ΔΔΔ*dcaP* were carboxylic acids,
146 including simple carboxylic acids, hydroxy carboxylic acids, and sugar acids (Fig. 3A-B).
147 Conversely, compounds in which the mutant outgrew WT were largely amino acids and their
148 derivatives (Fig. 3A-B). These data suggest that DcaP porins may allow the influx of carboxylic
149 acid-containing compounds, as previously predicted (20).
150
151 *DcaP3 is important for growth on multiple carboxylic acid carbon sources*
152 To verify the Biolog results and further determine specificity of the DcaP classes, growth
153 curves using ΔΔΔ*dcaP,* Δ*dcaP1*Δ*dcaP2*, Δ*dcaP1*Δ*dcaP3*, and Δ*dcaP2*Δ*dcaP3* and the carboxylic
154 acids as sole carbon sources were performed. Mutants lacking DcaP3 were defective for growth
155 on citric acid, tricarballylic acid, and mucic acid compared to the wild-type strain (Fig. 4A). We
156 were unable to identify conditions in which DcaP1 or DcaP2 were required for growth.
157 Complementation experiments showed that DcaP3 expression was sufficient to restore growth
158 on these substrates to near wild-type levels (Fig. 4B). Similarly, a single Δ*dcaP3* mutation

159 conferred a defect in growth on citric acid, tricarballylic acid, and mucic acid, whereas single
160 mutants of Δ*dcaP1* or Δ*dcaP2* showed no defect (Fig. S3).
161 A recent study in *A. baylyi* found that tricarballylic acid metabolism is closely linked with
162 the metabolism of *cis*- and *trans*-aconitic acid (33). The genetic organization of the tricarballylic
163 acid catabolic genes are conserved in *A. baumannii* compared to *A. baylyi* (Fig. 4C). Since the
164 data thus far suggest DcaP3 is necessary for growth on tricarballylic acid, we hypothesized that
165 DcaP3 may also be important for *cis*- and *trans*-aconitic acid growth. Mutants lacking DcaP3
166 had a defect for growth on both *cis*- and *trans*-aconitic acid (Fig. 4A). Complementing DcaP3 in
167 the chromosome of the triple mutant ΔΔΔ*dcaP* restored growth to near wild-type-like levels,
168 confirming the role of DcaP3 in growth on these carbon sources (Fig. 4B). Finally, the Δ*dcaP3*
169 single mutant had a defect in growth on both *cis*- and *trans*-aconitic acid compared to wildtype
170 (Fig. S3). To highlight the similarities in the carbon sources in which DcaP3 is important for
171 growth, the chemical structures for each carbon source are outlined in Fig. 4D. Taken together,
172 these data suggest that DcaP3 is important for growth using multiple di- and tri-carboxylic acids
173 as sole carbon sources.
174
175 *DcaP4 complements Δ*dcaP3 for growth on carboxylic acids*
176 Thus far, experiments were performed with *A. baumannii* ATCC 17978 which does not
177 encode DcaP4; thus, the potential role for DcaP4 in growth using carboxylic acids was unclear.
178 *A. baylyi* can grow on citric acid and tricarballylic acid and does not encode DcaP3 but rather
179 DcaP1, DcaP2, and DcaP4 (33). We hypothesized that DcaP4 could be also allow influx of
180 carboxylic acids. To test this, the DcaP4 from *A. baumannii* AB5075, which shares 77% amino
181 acid identity to *A. baylyi* DcaP4, was expressed from the 17978 DcaP3 promoter in the
182 ΔΔΔ*dcaP A. baumannii* mutant. Consistent with previous observations, the ΔΔΔ*dcaP* mutant was
183 unable to grow using citric acid, tricarballylic acid, mucic acid, or *cis*- and *trans*-aconitic acid

184 (Fig. 5). Growth was restored to the ΔΔΔ*dcaP* mutant by expressing DcaP4 chromosomally from
185 the DcaP3 promoter, suggesting that DcaP4 and DcaP3 have overlapping functions in some *A.*
186 *baumannii* strains (Fig. 5).
187
188 *DcaP3 is required for growth on di- and tri- carboxylic acids in a clinical isolate*
189 To test if DcaP3 is important for growth on di- and tri-carboxylic acids in a more recent
190 clinical isolate, a Δ*dcaP3* mutant was generated in the more recent clinical isolate AB5075 and
191 similar growth curves were performed. Mutants lacking *dcaP3* were defective for growth on citric
192 acid, tricarballylic acid, mucic acid, and *cis*- and *trans*-aconitic acid compared to wild-type (Fig.
193 6). This suggests that the requirement for DcaP3 for growth on select carboxylic acids as sole
194 carbon sources is conserved among *A. baumannii* isolates.
195
196 *DcaP3 is required for virulence in the liver and spleen during bloodstream infection of mice*
197 Carbon source utilization can be a critical determinant of pathogenesis for *A. baumannii*
198 and other bacterial species in different host niches (34,35). Therefore, we sought to determine if
199 DcaP function is important for *A. baumannii* pathogenesis. To test this, murine bloodstream
200 infections were performed, co-inoculating wild-type and the ΔΔΔ*dcaP* mutant or wild-type and
201 the ΔΔΔ*dcaP* mutant complemented with DcaP3. We hypothesized that there may be a host
202 niche in which DcaP proteins are important for *A. baumannii* replication, leading to a defect for
203 ΔΔΔ*dcaP* compared to wildtype. There was no defect of the ΔΔΔ*dcaP* mutant compared to
204 wildtype in lung, kidney, or heart (Fig. 7A). By contrast, there was a defect for the ΔΔΔ*dcaP*
205 mutant compared to wildtype in the spleen and liver (Fig. 7A). The defect in the spleen and liver
206 was reversed by complementing *dcaP3* in the chromosome of the ΔΔΔ*dcaP* mutant, showing
207 DcaP3 is important for replication in the liver and spleen (Fig. 7B). Together these data suggest
208 that carboxylic acid permeability by DcaP3 is important in specific host niches during infection.
209

210 **DISCUSSION**

211 The OM protects *A. baumannii* from antimicrobials and other host stresses but must
212 permit influx of nutrients essential for replication. How nutrients pass through the *A. baumannii*
213 OM is not well understood. Here, we designate classes of a family of predicted porins, DcaP1-4,
214 that are widely distributed across *Acinetobacter spp.* and show DcaP3 or DcaP4 are required for
215 growth on multiple carboxylic acids.

216 DcaP-like porins have been identified in genetic screens for biofilm formation,
217 desiccation, and mucin catabolism, largely referred to as DcaP-like proteins without further
218 distinction (26,27,36–38). We show that *A. baumannii* DcaP-like proteins can be grouped into
219 four classes based on protein sequence (Fig. 1A, S1A). The presence of DcaP-encoding genes
220 is conserved among *Acinetobacter* spp, and particularly in *A. baumannii* and the *acb* complex
221 (Fig. 1B, Fig. S1B). While DcaP proteins can be found in distantly related organisms (Fig. 2A),
222 the DcaP1-4 classes we define in *A. baumannii* cluster together (Fig. 2B). These findings
223 suggest DcaP1-4 diversified within the *Acinetobacter* clade.

224 Antibiotic resistance in *A. baumannii* is a critical public health problem due to the
225 emergence of XDR isolates. Various porins in *A. baumannii* have been implicated in the uptake
226 of toxic molecules including antibiotics (12,39–41). DcaP3 was proposed to allow entry for the
227 beta-lactamase inhibitor sulbactam (21). Here, we show encoding DcaP-like proteins has no
228 impact on sensitivity to ampicillin in the presence of sulbactam under the conditions tested (Fig.
229 S2). These data suggest DcaP-like proteins may not be required for function of sulbactam.

230 The transport of essential nutrients across the cell envelope is incompletely understood
231 in *A. baumannii*. In general, *A. baumannii* utilizes organic acids and amino acids as carbon
232 sources and cannot utilize sugars such as glucose (34). Accordingly, multiple OM channels
233 have been identified that are important for growth on specific carbon sources including ornithine,
234 arginine, glutamic acid, and benzoic acid (16–19,42). One study in ATCC 19606 found that
235 DcaP1 (*A1S_1380*) was upregulated in the presence of mucin, suggesting DcaP1 may play a

236 role in the influx of mucin components (26). In a Biolog screen, we identified multiple carboxylic
237 acid carbon sources that supported significantly more growth of the wildtype compared to the
238 ΔΔΔ*dcaP* mutant (Fig. 3), suggesting DcaP-family proteins are important for their diffusion
239 through the OM.

240 The data suggest DcaP3 is responsible for the influx of carboxylic acid carbon sources
241 citric acid, mucic acid, tricarballylic acid, and *cis*- and *trans*- aconitic acid in *A. baumannii* ATCC
242 17978, as mutants lacking DcaP3 show decreased growth on these substrates (Fig. 4A-B, S3).
243 However, the Δ*dcaP3* mutant grew more than the ΔΔΔ*dcaP* mutant in ATCC 17978, suggesting
244 DcaP1 or DcaP2 may play a minor role in growth with these carbon sources (Fig. S3). Citric
245 acid is an intermediate of the tricarboxylic acid (TCA) cycle, a ubiquitous pathway for energy
246 generation. Despite this, many bacteria cannot utilize citric acid as a carbon source and how
247 citric acid permeates the OM is unknown (43). Mutants in *P. aeruginosa* OpdH were defective
248 for growth on *cis*-aconitic acid, but not on citric acid, suggesting they encode other citric acid
249 transporters (44,45). A ΔΔΔ*dcaP* mutant displayed a strong defect for growth on citric acid that
250 can be rescued by complementing with DcaP3 or DcaP4 (Fig. 4A, 4B, Fig. 5). Therefore,
251 encoding multiple porins for OM citric acid passage may be conserved across bacterial genera.

252 Mucic acid, or galactaric acid, is a sugar acid derived from the oxidation of galactose and
253 is unrelated to mucin. Mucic acid is not typically found in the host; but, some antibiotic
254 treatments result in increased mucic acid in the human gut (46–48). However, only a subset of
255 *A. baumannii* strains, including ATCC 17978, encode the D-galactaric acid dehydrogenase
256 required for growth on mucic acid (49). The digestive tract is a reservoir for *A. baumannii*
257 colonization that increases the potential for infection and transmission and *A. baumannii* ATCC
258 17978 can asymptomatically colonize the mouse gut (50–55). Thus, mucic acid may be used as
259 carbon source by some *A. baumannii* in the inflamed gut. Our data suggest that DcaP3 or
260 DcaP4 are important for growth on mucic acid.

261 The catabolism of *cis*- and *trans*-aconitic acid has been described in *A. baylyi*, and the
262 catabolism of tricarballylic acid in *A. baylyi* and *Salmonella* (33,56,57). However, the OM porin
263 required for growth on these carbon sources in *Acinetobacter* is unknown. Our data suggest that
264 DcaP3 or DcaP4 are important for growth on tricarballylic acid, and *cis*- and *trans*-aconitic acid.
265 Taken together, our data suggests that DcaP3 and DcaP4 are the major porins for passive
266 transport of specific carboxylic acid carbon sources.

267 The requirement for DcaP3 in growth on select di- and tri-carboxylic acids is conserved
268 in the more recent clinical isolate *A. baumannii* AB5075, as a Δ*dcaP3* mutant has reduced
269 growth in these conditions (Fig. 6). However, this was surprising as *A. baumannii* AB5075
270 encodes all four DcaP proteins, including DcaP4, which complemented growth in an *A.*
271 *baumannii* ATCC 17978 ΔΔΔ*dcaP* mutant (Fig. 5). We speculate that *dcaP4* may not be
272 expressed under these conditions.

273 During infection, bacteria must scavenge nutrients from the host to replicate. The *A.*
274 *baumannii* ATCC 17978 ΔΔΔ*dcaP* mutant had a defect compared to wildtype in the mouse liver
275 and spleen that was complemented by expression of *dcaP3* (Fig. 7A-B). This suggests DcaP3
276 passive import of carboxylic acid carbon sources is important for pathogenesis in the liver and
277 spleen. Alternatively, DcaP3 may play another role in pathogenesis. For example, porins in *A.*
278 *baumannii* have demonstrated roles for the adhesion or invasion of eukaryotic cells (13,58–61).
279 DcaP3 is the DcaP-like protein that is a proposed vaccine candidate (21–25). These data
280 suggest that neutralizing DcaP3 may also promote *A. baumannii* clearance.

281 In summary, we further classify a family of porins previously termed DcaP-like into four
282 classes in *Acinetobacter* spp. This classification allows for the differentiation between DcaP-like
283 proteins and the potential to determine individual functions for DcaP1-4 in *Acinetobacter* spp.
284 DcaP3 was critically important for growth on citric acid, tricarballylic acid, mucic acid, and *cis*-
285 and *trans*-aconitic acid as sole carbon sources. A ΔΔΔ*dcaP* mutant was attenuated in a
286 competitive murine systemic infection and complemented by expression of DcaP3, suggesting a

287 role for DcaP3 in pathogenesis and validating its potential as a therapeutic target. Our data
288 therefore provides a deeper understanding of how *A. baumannii* acquires nutrients including in
289 the host.
290
291
292 **MATERIALS AND METHODS**
293 Bacterial strain construction and growth
294 All bacterial strains and plasmids used in this study are listed in Tables S1 and S2,
295 respectively. The wild-type strain was *A. baumannii* ATCC 17978VU or AB5075 (62).
296 Oligonucleotides are listed in Table S3 and were purchased from Integrated DNA Technologies
297 (Coralville, IA). Strains were grown in Luria-Bertani lysogeny broth (LB; Miller) or on LB with
298 1.5% (wt/vol) agar unless indicated otherwise. Antibiotics were used at the following
299 concentrations: carbenicillin (Carb), 75 mg/L; kanamycin (Kan), 40 mg/L; chloramphenicol, 15
300 mg/L; hygromycin (Hyg) 300 mg/L. For deletion constructs, 1000 bp of 3' and 5' flanking DNA to
301 the gene of interest was amplified using Q5 High Fidelity 2x Master Mix [New England Biolabs
302 (NEB), Ipswich, MA] from *A. baumannii* ATCC 17978VU or AB5075. The vector pFLP2 was
303 digested with BamHI and KpnI restriction enzymes (NEB, Ipswitch, MA) and gel purified. The
304 kanamycin or hygromycin cassette was amplified from pKD4. Fragments were ligated together
305 using HiFi ligation mix (NEB, Ipswitch, MA), transformed into chemically competent *E. coli*
306 DH5α, and plated to selective media. Transformants were confirmed to contain the insert by
307 PCR. To generate the knockout strains, a triparental conjugation using helper *E. coli* strain
308 HB101 containing pRK2013 was performed. Single-crossover merodiploids containing the
309 integrated pFLP2 vector were chosen based on a Kan^R $Carb^R$ or Hyg^R and sucrose-sensitive
310 (10% w/v; Suc^S) phenotype. Putative merodiploids displaying were verified by PCR.
311 Merodiploids were then grown on LB agar, resuspended, and plated to LB agar or LB agar with

312 10% sucrose to select for colonies with the second crossover event. Colonies were then
313 screened for a Kan^R $Carb^S$ Suc^R or Hyg^R Suc^S phenotype. Mutants were confirmed via PCR.
314 For chromosomal integration constructs, DNA from ATCC 17978VU or AB5075 was
315 amplified using Q5 High Fidelity 2x Master Mix (NEB, Ipswich, MA). The mTn7 pKNOCK vector
316 was digested with BamHI and KpnI prior to ligation using HiFi ligation mix (NEB, Ipswitch, MA)
317 and transformation into chemically competent *E. coli* DH5α λ*pir116*$^+$. To generate
318 chromosomally integrated mTn7 constructs, a modified four-way parental mating was performed
319 using helper *E. coli* strain HB101 containing pRK2013 and *E. coli* DH5α containing pTNS2 (63).
320 Colonies were screened by PCR for integration into the correct chromosomal locus at the *att*
321 site. All plasmid constructs were verified by whole plasmid sequencing before transforming into
322 *A. baumannii* (Plasmidsaurus, South San Francisco, CA).
323
324 Phylogenetic tree construction
325 To identify DcaP orthologs and classify them into hierarchical orthogroups (HOGs),
326 OrthoFinder v2.5.5 was used (64). Two datasets were analyzed: (i) a 253-strain dataset
327 including 235 *A. baumannii* strains deduplicated as previously described (65); (ii) a 28-species
328 dataset that included multiple *Acinetobacter* and a broader range of gammaproteobacteria
329 rooted by one alphaproteobacterial. The protein accession numbers and genome accession
330 numbers are listed in Table S4.
331 Non-Acinetobacter species were selected based on the conservation of DcaP orthologs
332 across the genus or species indicated by KEGG. Specific organisms were selected to portray a
333 representative distribution of DcaP orthologs across bacteria, a group of 22 species. The
334 FastTree v2.1.11-derived (66), manually rooted species tree was used as an input for
335 OrthoFinder HOG inference (64,67), ensuring accurate classification of gene duplication and
336 speciation events. The resulting DcaP classifications were visualized and annotated in iTOL

337 (68). To infer a species phylogeny, a set of 120 universal bacterial marker genes (Bac120) was
338 identified from each proteome using HMMER3 (hmmsearch, v3.3), following the methodology
339 described in Parks *et al*. 2018 (69). The majority of species had only one significant hit for each
340 of the 120 protein HMMs; if a species had more than one hit, the best-scoring hit for that marker
341 was extracted.

342 Each of the 120 marker proteins was independently aligned to its respective HMM profile
343 using hmmalign (HMMER v3.3). Alignments were trimmed to remove poorly aligned regions and
344 concatenated into a single concatenated supermatrix for each species. To improve alignment
345 quality, columns were filtered based on the following criteria: (i) highly gapped regions (>80%
346 gaps) were removed; (ii) completely homogenous columns were excluded to reduce
347 redundancy.

348 Maximum likelihood species trees were inferred from the filtered concatenated alignment
349 using FastTree v2.1.11, with the LG model of amino acid evolution. The resulting unrooted trees
350 were manually rooted and annotated in iTOL using *Brevundimonas subvibrioides* or *E.coli* as
351 outgroups for the smaller and larger datasets.

352

353 <u>DcaP protein phylogeny</u>

354 DcaP homologs were extracted from their respective proteomes by selecting sequences
355 within the DcaP HOG at the root of all *Acinetobacter* species in the 255-species dataset in
356 Orthofinder. To ensure consistent domain identification, sequences were aligned to the Pfam
357 Hidden Markov Model (HMM) PF19577.4, corresponding to the DcaP OM protein family.
358 Alignments were trimmed to remove poorly aligned residues prior to phylogenetic inference. A
359 maximum likelihood phylogenetic tree was constructed using FastTree v2.1.11 with the LG
360 model of amino acid evolution. The inferred clusters were identical to OrthoFinder's DcaP
361 subfamilies, except for a small cluster of DcaP proteins that OrthoFinder grouped with DcaP1,
362 while FastTree grouped the same cluster with DcaP3.

363 To identify putative orthologs of DcaP proteins from the 22 species identified above and
364 *A. baumannii* AB5075, proteomes from genomic assemblies were downloaded from the NCBI
365 Datasets database. Two complementary approaches were employed to verify orthology. First,
366 HMMER v3.4 was used to search each proteome with the Pfam profile HMM PF19577,
367 corresponding to the DcaP protein family. Significant hits were retained as candidate DcaP
368 homologs. To independently assess orthology and reconstruct gene relationships, OrthoFinder
369 v2.5.5 was run on all 23 proteomes, which also produced a rooted gene tree for the DcaP
370 family. The resulting DcaP sequences were realigned to the PF19577 HMM using hmmalign,
371 and poorly aligned or unaligned amino acids were trimmed. A maximum likelihood phylogeny
372 was then inferred using RAxML v8.2.12, under the LG amino acid substitution model.
373 Amino acid sequence alignment and percent identity were determined using the Clustal
374 Omega program (28).
375
376
377 Carbon source utilization screen using Biolog plates
378 Plates PM1 and PM2A were obtained from Biolog for carbon source utilization testing. A
379 110 μL aliquot of defined M9 minimal media lacking carbon was dispensed into every well and
380 resuspended. Then, 100 μL was transferred from the Biolog plates into sterile flat-bottom 96-
381 well plates. Overnight bacterial cultures were diluted 100-fold in sterile PBS before 1 μL of
382 diluted culture was inoculated into every well. Plates were incubated at 37°C with shaking and
383 growth was monitored by optical density at 600 nm (OD_{600}) in an EPOCH2 or SynergyH1 BioTek
384 plate reader (Winooski, VT). Background absorbance was subtracted before area under the
385 curve calculations for each isolate and each compound were calculated and the difference
386 between wildtype and ΔΔΔ*dcaP* was analyzed. Compounds were included if any isolate of
387 either wildtype or ΔΔΔ*dcaP* reached an OD_{600} of 0.15 or higher.

388

389 Growth curve analyses

390 M9 minimal medium without glucose was supplemented 0.1X Vishniac's trace minerals
391 (70) with the specified carbon source at a concentration to maintain the carbon equivalency of a
392 4-carbon compound at 16.5 mM. Cultures were inoculated with a single bacterial colony and
393 grown in 3 mL LB media overnight at 37°C with shaking at 180 rpm for 8-16 hours. Growth
394 curves were performed by diluting overnight cultures 100-fold in sterile PBS and inoculating 1
395 μL diluted culture into 99 μL media in a 96-well flat bottom plate. Growth was monitored as
396 described above.

397

398 Murine bloodstream infection

399 Six-week-old female ND4 Swiss Webster mice were purchased from Envigo/Harlan
400 Laboratory. Mice were boarded in a temperature-controlled environment with 14:10 h light:dark
401 cycles and food and water were provided as needed. Mice were acclimated to the facility for 1
402 week prior to infection. Mice were anesthetized with isoflurane and inoculated retro-orbitally with
403 approximately 3×10^8 CFU in a 50 μL bacterial suspension of a 1:1 mixture of *A.*
404 *baumannii* ATCC 17978VU wildtype and ΔΔΔ*dcaP* mutant or ΔΔΔ*dcaP*+*dcaP3*. For wildtype
405 versus ΔΔΔ*dcaP,* 5 of the mice were infected with wild-type ATCC 17978VU and 5 were infected
406 with ATCC 17978 mTn7(Carb^R). All mice infected with the complement strain were infected with
407 ATCC 17978VU. The inoculum dose was determined by serial dilution and plating on selective
408 agar media. Mice were euthanized at 24 h post infection by CO_2 asphyxiation, and the organs
409 were excised aseptically. Tissues were homogenized in PBS using a Bullet Blender (Next
410 Advance, Troy, NY), and all samples were serially diluted and plated on LB and LB with
411 carbenicillin or kanamycin selective agar plates for bacterial enumeration. All animal care
412 protocols were approved by the University of Illinois Chicago Institutional Animal Care and Use

Committee (IACUC; protocol number 23–119) in accordance with the Animal Care Policies of UIC, the Animal Welfare Act, the National Institutes of Health, and the American Veterinary Medical Association (AVMA). Animals were humanely euthanized consistent with the AVMA guidelines.

Data reporting, statistical analysis, and figure preparation

Each measurement was taken from a distinct biological sample (e.g., bacterial culture from a single colony or an individual mouse). Data processing and statistical analyses were performed using Microsoft Excel 16.98 and GraphPad Prism 10.4.2. Statistical tests used are indicated in each figure legend. Figures were prepared in Adobe Illustrator 25.2.3.

Author contributions

H.R.N. – project conceptualization, methodology, data collection, data analysis, and writing. J.D.W – bioinformatics, data analysis, and writing. L.D.P. – project conceptualization, methodology, data analysis, writing, funding, and resources.

ACKNOWLEDGMENTS

We thank the members of the Palmer laboratory for critical reading of the manuscript and The Michael Reese Research and Education Foundation Pioneer in Research Award for funding.

433 **REFERENCES**
434

435 1. Clark NM, Zhanel GG, Lynch JPI. Emergence of antimicrobial resistance among
436 *Acinetobacter* species: a global threat. Curr Opin Crit Care. 2016 Oct;22(5):491.

437 2. World Health Organization. No time to wait: securing the future from drug-resistant
438 infections. World Health Organization and Interagency Coordination Group on Antimicrobial
439 Resistance; 2019 Apr.

440 3. Weiner LM, Webb AK, Limbago B, Dudeck MA, Patel J, Kallen AJ, et al. Antimicrobial-
441 resistant pathogens associated with healthcare-associated infections: summary of data
442 reported to the National Healthcare Safety Network at the Centers for Disease Control and
443 Prevention, 2011–2014. Infect Control Hosp Epidemiol. 2016 Nov;37(11):1288–301.

444 4. Tacconelli E, Carrara E, Savoldi A, Harbarth S, Mendelson M, Monnet DL, et al. Discovery,
445 research, and development of new antibiotics: the WHO priority list of antibiotic-resistant
446 bacteria and tuberculosis. Lancet Infect Dis. 2018 Mar 1;18(3):318–27.

447 5. Silhavy TJ, Kahne D, Walker S. The bacterial cell envelope. Cold Spring Harb Perspect Biol.
448 2010 May;2(5):a000414.

449 6. Nikaido H. Molecular basis of bacterial outer membrane permeability revisited. Microbiol Mol
450 Biol Rev. 2003 Dec;67(4):593–656.

451 7. Geisinger E, Huo W, Hernandez-Bird J, Isberg RR. *Acinetobacter baumannii*: envelope
452 determinants that control drug resistance, virulence, and surface variability. Annu Rev
453 Microbiol. 2019;73(1):481–506.

454 8. Kenyon JJ, Hall RM. Variation in the complex carbohydrate biosynthesis loci of
455 *Acinetobacter baumannii* genomes. PLOS ONE. 2013 Apr 16;8(4):e62160.

456 9. Kenyon JJ, Nigro SJ, Hall RM. Variation in the OC locus of *Acinetobacter baumannii*
457 genomes predicts extensive structural diversity in the lipooligosaccharide. PLOS ONE. 2014
458 Sep 23;9(9):e107833.

459 10. Silale A, Berg B van den. TonB-dependent transport across the bacterial outer membrane.
460 Annu Rev Microbiol. 2023 Sep 15;77(Volume 77, 2023):67–88.

461 11. Sugawara E, Nikaido H. OmpA is the principal nonspecific slow porin of *Acinetobacter*
462 *baumannii*. J Bacteriol. 2012 Jul 18;194(15):4089–96.

463 12. Iyer R, Moussa SH, Durand-Réville TF, Tommasi R, Miller A. *Acinetobacter baumannii*
464 OmpA Is a selective antibiotic permeant porin. ACS Infect Dis. 2018 Mar 9;4(3):373–81.

465 13. Scribano D, Cheri E, Pompilio A, Di Bonaventura G, Belli M, Cristina M, et al. *Acinetobacter*
466 *baumannii* OmpA-like porins: functional characterization of bacterial physiology, antibiotic-
467 resistance, and virulence. Commun Biol. 2024 Aug 6;7(1):1–11.

468 14. Samsudin F, Ortiz-Suarez ML, Piggot TJ, Bond PJ, Khalid S. OmpA: a flexible clamp for
469 bacterial cell wall attachment. Structure. 2016 Dec 6;24(12):2227–35.

470 15. Park JS, Lee WC, Yeo KJ, Ryu KS, Kumarasiri M, Hesek D, et al. Mechanism of anchoring
471 of OmpA protein to the cell wall peptidoglycan of the gram-negative bacterial outer
472 membrane. FASEB J. 2012 Jan;26(1):219.

473 16. Mussi MA, Relling VM, Limansky AS, Viale AM. CarO, an *Acinetobacter baumannii* outer
474 membrane protein involved in carbapenem resistance, is essential for l-ornithine uptake.
475 FEBS Lett. 2007;581(29):5573–8.

476 17. Zahn M, Bhamidimarri SP, Baslé A, Winterhalter M, van den Berg B. Structural insights into
477 outer membrane permeability of *Acinetobacter baumannii*. Structure. 2016 Feb 2;24(2):221–
478 31.

479 18. Clark TJ, Momany C, Neidle EL. The *benPK* operon, proposed to play a role in transport, is
480 part of a regulon for benzoate catabolism in *Acinetobacter* sp. strain ADP1. Microbiology.
481 2002;148(4):1213–23.

482 19. Smith MA, Weaver VB, Young DM, Ornston LN. Genes for chlorogenate and
483 hydroxycinnamate catabolism (hca) are linked to functionally related genes in the *dca-pca-*
484 *qui-pob-hca* chromosomal cluster of *Acinetobacter* sp. strain ADP1. Appl Environ Microbiol.
485 2003 Jan;69(1):524–32.

486 20. Parke D, Garcia MA, Ornston LN. Cloning and genetic characterization of *dca* genes
487 required for β-oxidation of straight-chain dicarboxylic acids in *Acinetobacter* sp. strain ADP1.
488 Appl Environ Microbiol. 2001 Oct;67(10):4817–27.

489 21. Bhamidimarri SP, Zahn M, Prajapati JD, Schleberger C, Söderholm S, Hoover J, et al. A
490 multidisciplinary approach toward identification of antibiotic scaffolds for *Acinetobacter*
491 *baumannii*. Structure. 2019 Feb 5;27(2):268-280.e6.

492 22. Raoufi Z, Abdollahi S, Armand R. DcaP porin and its epitope-based subunit promise
493 effective vaccines against *Acinetobacter baumannii*; *in-silico* and *in-vivo* approaches. Microb
494 Pathog. 2022 Jan;162:105346.

495 23. Fereshteh S, Ajdary S, Sepehr A, Bolourchi N, Barzi SM, Haririzadeh Jouriani F, et al.
496 Immunization with recombinant DcaP-like protein and AbOmpA revealed protections against
497 sepsis infection of multi-drug resistant *Acinetobacter baumannii* ST2Pas in a C57BL/6
498 mouse model. Microb Pathog. 2023 Jan;174:105882.

499 24. Khalid K, Irum S, Ullah SR, Andleeb S. In-silico vaccine design based on a novel vaccine
500 candidate against infections caused by *Acinetobacter baumannii*. Int J Pept Res Ther. 2021
501 Dec 2;28(1):16.

502 25. Fereshteh S, Abdoli S, Shahcheraghi F, Ajdary S, Nazari M, Badmasti F. New putative
503 vaccine candidates against *Acinetobacter baumannii* using the reverse vaccinology method.
504 Microb Pathog. 2020 Jun 1;143:104114.

505 26. Ohneck EJ, Arivett BA, Fiester SE, Wood CR, Metz ML, Simeone GM, et al. Mucin acts as a
506 nutrient source and a signal for the differential expression of genes coding for cellular
507 processes and virulence factors in *Acinetobacter baumannii*. PLoS ONE. 2018 Jan
508 8;13(1):e0190599.

509 27. Cabral MP, Soares NC, Aranda J, Parreira JR, Rumbo C, Poza M, et al. Proteomic and
510 functional analyses reveal a unique lifestyle for *Acinetobacter baumannii* biofilms and a key
511 role for histidine metabolism. J Proteome Res. 2011 Aug 5;10(8):3399–417.

512 28. Sievers F, Wilm A, Dineen D, Gibson TJ, Karplus K, Li W, et al. Fast, scalable generation of
513 high-quality protein multiple sequence alignments using Clustal Omega. Mol Syst Biol. 2011
514 Oct 11;7:539.

515 29. Kanehisa M, Goto S. KEGG: kyoto encyclopedia of genes and genomes. Nucleic Acids Res.
516 2000 Jan 1;28(1):27–30.

517 30. Kanehisa M, Furumichi M, Sato Y, Matsuura Y, Ishiguro-Watanabe M. KEGG: biological
518 systems database as a model of the real world. Nucleic Acids Res. 2025 Jan
519 6;53(D1):D672–7.

520 31. Ji J, Du X, Chen Y, Fu Y, Wang H, Yu Y. In vitro activity of sulbactam in combination with
521 imipenem, meropenem, panipenem or cefoperazone against clinical isolates of
522 *Acinetobacter baumannii*. Int J Antimicrob Agents. 2013 Apr 1;41(4):400–1.

523 32. Choi JY, Soo Park Y, Cho CH, Seon Park Y, Shin SY, Song YG, et al. Synergic in-vitro
524 activity of imipenem and sulbactam against *Acinetobacter baumannii*. Clin Microbiol Infect.
525 2004 Dec 1;10(12):1098–101.

526 33. Baugh AC, Defalco JB, Duscent-Maitland CV, Tumen-Velasquez MP, Laniohan NS, Figatner
527 K, et al. Regulation of tricarboxylate transport and metabolism in *Acinetobacter baylyi* ADP1.
528 Appl Environ Microbiol. 2024 Jan 30;90(2):e02111-23.

529 34. Ren X, Palmer LD. *Acinetobacter* metabolism in infection and antimicrobial resistance.
530 Infect Immun. 2023 May 16;91(6):e00433-22.

531 35. Barber MF, Fitzgerald JR. Mechanisms of host adaptation by bacterial pathogens. FEMS
532 Microbiol Rev. 2024 Jul 1;48(4):fuae019.

533 36. Rumbo-Feal S, Gómez MJ, Gayoso C, Álvarez-Fraga L, Cabral MP, Aransay AM, et al.
534 Whole transcriptome analysis of *Acinetobacter baumannii* assessed by RNA-sequencing
535 reveals different mRNA expression profiles in biofilm compared to planktonic cells. PLoS
536 ONE. 2013 Aug 30;8(8):e72968.

537 37. Shin JH, Lee HW, Kim SM, Kim J. Proteomic analysis of *Acinetobacter baumannii* in biofilm
538 and planktonic growth mode. J Microbiol. 2009 Dec 1;47(6):728–35.

539 38. Gayoso CM, Mateos J, Méndez JA, Fernández-Puente P, Rumbo C, Tomás M, et al.
540 Molecular mechanisms involved in the response to desiccation stress and persistence in
541 *Acinetobacter baumannii*. J Proteome Res. 2014 Feb 7;13(2):460–76.

542 39. Liu J, Chen S, Zhao B, Li G, Ma T. A novel FadL homolog, AltL, mediates transport of long-
543 chain alkanes and fatty acids in *Acinetobacter venetianus* RAG-1. Appl Environ Microbiol.
544 2022 Sep 28;88(20):e01294-22.

545 40. Mussi MA, Limansky AS, Viale AM. Acquisition of resistance to carbapenems in multidrug-
546 resistant clinical strains of *Acinetobacter baumannii*: natural insertional inactivation of a

547 gene encoding a member of a novel family of β-barrel outer membrane proteins. Antimicrob
548 Agents Chemother. 2005 Apr;49(4):1432–40.

549 41. Catel-Ferreira M, Coadou G, Molle V, Mugnier P, Nordmann P, Siroy A, et al. Structure-
550 function relationships of CarO, the carbapenem resistance-associated outer membrane
551 protein of *Acinetobacter baumannii*. J Antimicrob Chemother. 2011 Sep;66(9):2053–6.

552 42. Zahn M, D'Agostino T, Eren E, Baslé A, Ceccarelli M, van den Berg B. Small-molecule
553 transport by CarO, an abundant eight-stranded β-Barrel outer membrane protein from
554 *Acinetobacter baumannii*. J Mol Biol. 2015 Jul 17;427(14):2329–39.

555 43. Blount ZD, Borland CZ, Lenski RE. Historical contingency and the evolution of a key
556 innovation in an experimental population of Escherichia coli. Proc Natl Acad Sci U S A. 2008
557 Jun 10;105(23):7899–906.

558 44. Tamber S, Ochs MM, Hancock REW. Role of the novel OprD family of porins in nutrient
559 uptake in *Pseudomonas aeruginosa*. J Bacteriol. 2006 Jan;188(1):45–54.

560 45. Tamber S, Maier E, Benz R, Hancock REW. Characterization of OpdH, a *Pseudomonas*
561 *aeruginosa* porin involved in the uptake of tricarboxylates. J Bacteriol. 2007
562 Feb;189(3):929–39.

563 46. Hwang I, Park YJ, Kim YR, Kim YN, Ka S, Lee HY, et al. Alteration of gut microbiota by
564 vancomycin and bacitracin improves insulin resistance via glucagon-like peptide 1 in diet-
565 induced obesity. FASEB J. 2015;29(6):2397–411.

566 47. Theriot CM, Koenigsknecht MJ, Carlson PE, Hatton GE, Nelson AM, Li B, et al. Antibiotic-
567 induced shifts in the mouse gut microbiome and metabolome increase susceptibility to
568 *Clostridium difficile* infection. Nat Commun. 2014;5:3114.

569 48. Faber F, Tran L, Byndloss MX, Lopez CA, Velazquez EM, Kerrinnes T, et al. Host-mediated
570 sugar oxidation promotes post-antibiotic pathogen expansion. Nature. 2016 Jun
571 30;534(7609):697–9.

572 49. Farrugia DN, Elbourne LDH, Hassan KA, Eijkelkamp BA, Tetu SG, Brown MH, et al. The
573 complete genome and phenome of a community-acquired *Acinetobacter baumannii*. PLOS
574 ONE. 2013 Mar 19;8(3):e58628.

575 50. Timsit JF, Garrait V, Misset B, Goldstein FW, Renaud B, Carlet J. The digestive tract is a
576 major site for *Acinetobacter baumannii* colonization in intensive care unit patients. J Infect
577 Dis. 1993 Nov 1;168(5):1336–7.

578 51. Corbella X, Pujol M, Ayats J, Sendra M, Ardanuy C, Domínguez MA, et al. Relevance of
579 digestive tract colonization in the epidemiology of nosocomial infections due to multiresistant
580 *Acinetobacter baumannii*. Clin Infect Dis. 1996 Aug 1;23(2):329–34.

581 52. Wong SC, Chen JHK, Chau PH, So SYC, AuYeung CHY, Yuen LLH, et al. Gastrointestinal
582 colonization of carbapenem-resistant *Acinetobacter baumannii*: what is the implication for
583 infection control? Antibiotics. 2022 Sep 22;11(10):1297.

584 53. Harris AD, Johnson JK, Pineles L, O'Hara LM, Bonomo RA, Thom KA. Patient-to-patient
585 transmission of *Acinetobacter baumannii* gastrointestinal colonization in the intensive care
586 unit. Antimicrob Agents Chemother. 2019 Jul 25;63(8):10.1128/aac.00392-19.

587 54. Zheng Y, Xu N, Pang J, Han H, Yang H, Qin W, et al. Colonization with extensively drug-
588 resistant *Acinetobacter baumannii* and prognosis in critically ill patients: an observational
589 cohort study. Front Med. 2021;8:667776.

590 55. Ren X, Clark RM, Bansah DA, Varner EN, Tiffany CR, Jaswal K, et al. Amino acid
591 competition shapes *Acinetobacter baumannii* gut carriage. BioRxiv Prepr Serv Biol. 2024
592 Oct 19;2024.10.19.619093.

593 56. Lewis JA, Stamper LW, Escalante-Semerena JC. Regulation of expression of the
594 tricarballylate utilization operon (*tcuABC*) of *Salmonella enterica*. Res Microbiol. 2009
595 Apr;160(3):179–86.

596 57. Lewis JA, Horswill AR, Schwem BE, Escalante-Semerena JC. The tricarballylate utilization
597 (*tcuRABC*) genes of *Salmonella enterica* serovar Typhimurium LT2. J Bacteriol. 2004
598 Mar;186(6):1629–37.

599 58. Gaddy JA, Tomaras AP, Actis LA. The *Acinetobacter baumannii* 19606 OmpA protein plays a
600 role in biofilm formation on abiotic surfaces and in the interaction of this pathogen with
601 eukaryotic cells. Infect Immun. 2009 Aug;77(8):3150–60.

602 59. Choi CH, Lee JS, Lee YC, Park TI, Lee JC. *Acinetobacter baumannii* invades epithelial cells
603 and outer membrane protein A mediates interactions with epithelial cells. BMC Microbiol.
604 2008 Dec 10;8:216.

605 60. Choi CH, Hyun SH, Lee JY, Lee JS, Lee YS, Kim SA, et al. *Acinetobacter baumannii* outer
606 membrane protein A targets the nucleus and induces cytotoxicity. Cell Microbiol.
607 2008;10(2):309–19.

608 61. Labrador-Herrera G, Pérez-Pulido AJ, Álvarez-Marín R, Casimiro-Soriguer CS, Cebrero-
609 Cangueiro T, Morán-Barrio J, et al. Virulence role of the outer membrane protein CarO in
610 carbapenem-resistant *Acinetobacter baumannii*. Virulence. 2020 Dec;11(1):1727–37.

611 62. Wijers CDM, Pham L, Menon S, Boyd KL, Noel HR, Skaar E, et al. Identification of two
612 variants of *Acinetobacter baumannii* 17978 with distinct genotypes and phenotypes. Infect
613 Immun. 2021 Aug 30;IAI0045421.

614 63. Kumar A, Dalton C, Cortez-Cordova J, Schweizer HP. Mini-Tn7 vectors as genetic tools for
615 single copy gene cloning in *Acinetobacter baumannii*. J Microbiol Methods. 2010
616 Sep;82(3):296–300.

617 64. Emms DM, Kelly S. OrthoFinder: phylogenetic orthology inference for comparative
618 genomics. Genome Biol. 2019 Nov 14;20(1):238.

619 65. Noel HR, Keerthi S, Ren X, Winkelman JD, Troutman JM, Palmer LD. Genetic synergy
620 between *Acinetobacter baumannii* undecaprenyl phosphate biosynthesis and the Mla
621 system impacts cell envelope and antimicrobial resistance. mBio. 2024 Feb
622 16;15(3):e02804-23.

623 66. Price MN, Dehal PS, Arkin AP. FastTree 2 – approximately maximum-likelihood trees for
624 large alignments. PLOS ONE. 2010 Mar 10;5(3):e9490.

625 67. Emms DM, Kelly S. OrthoFinder: solving fundamental biases in whole genome comparisons
626 dramatically improves orthogroup inference accuracy. Genome Biol. 2015 Aug 6;16(1):157.

627 68. Letunic I, Bork P. Interactive Tree Of Life (iTOL): an online tool for phylogenetic tree display
628 and annotation. Bioinforma Oxf Engl. 2007 Jan 1;23(1):127–8.

629 69. Parks DH, Chuvochina M, Waite DW, Rinke C, Skarshewski A, Chaumeil PA, et al. A
630 standardized bacterial taxonomy based on genome phylogeny substantially revises the tree
631 of life. Nat Biotechnol. 2018 Nov;36(10):996–1004.

632 70. Vishniac W, Santer M. The thiobacilli. Bacteriol Rev. 1957 Sep;21(3):195–213.

633

634

635 **FIGURES**

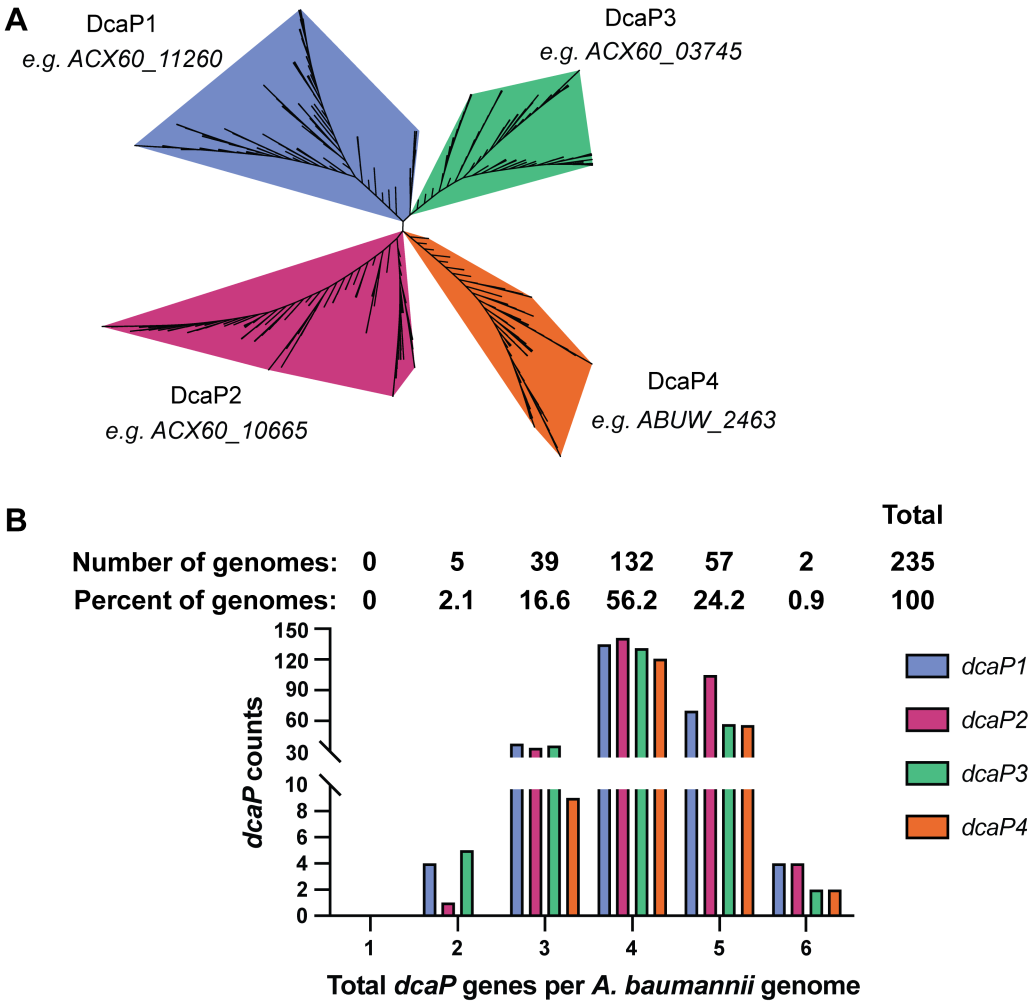

636
637 **Figure 1. *A. baumannii* DcaP proteins cluster in four classes and are widely distributed**
638 **among *Acinetobacter*. (A)** An unrooted tree of DcaP protein sequences from 255
639 *Acinetobacter* genomes (235 *A. baumannii* genomes). **(B)** Manual counts and distribution of
640 individual DcaP proteins binned by the total number of DcaP proteins in an *A. baumannii*
641 genome.
642

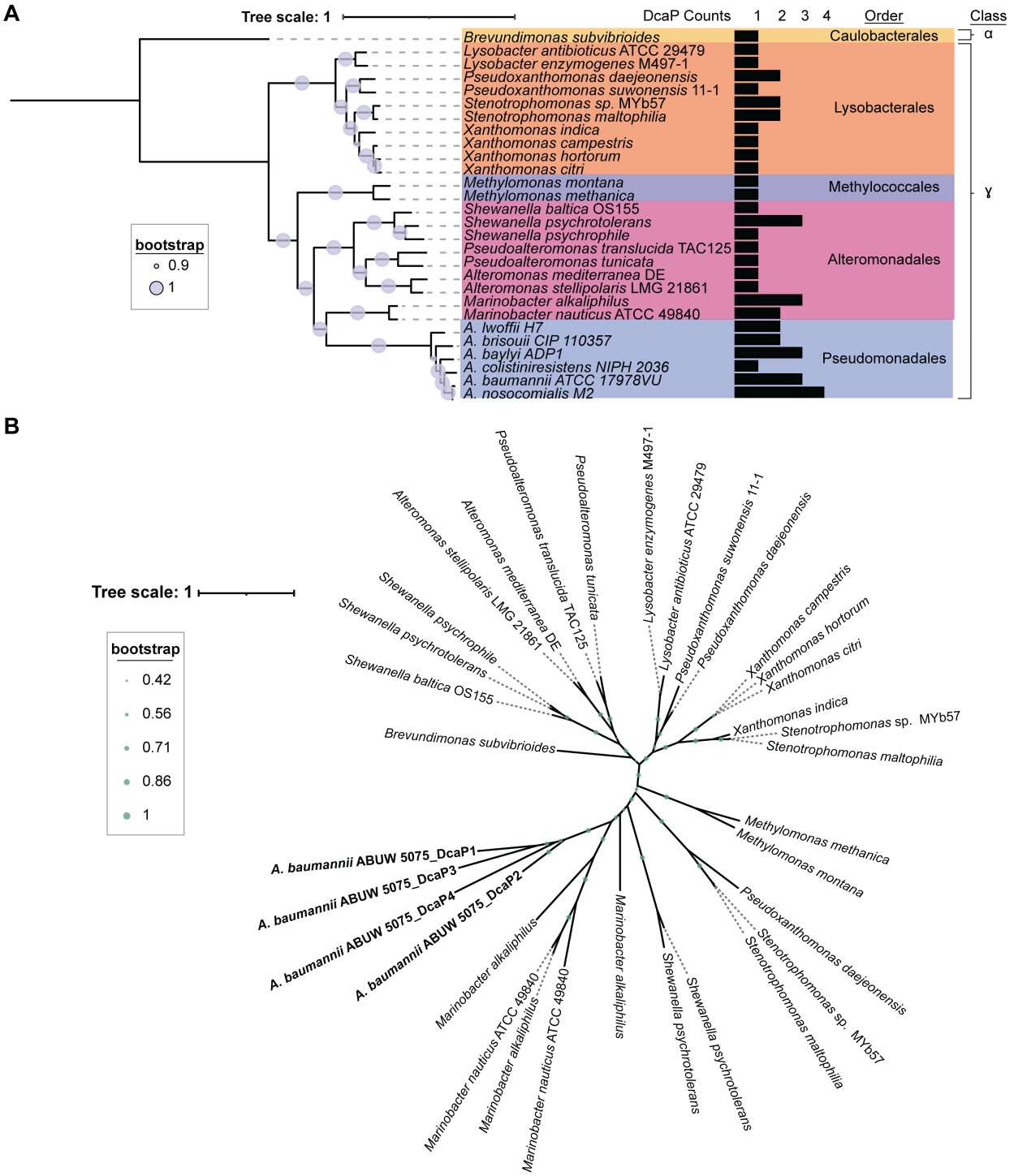

Figure 2. *A. baumannii* DcaP-family proteins cluster together compared to non-*Acinetobacter* DcaP proteins. (A) A rooted tree of DcaP containing species outside of *Acinetobacter* and some *Acinetobacter spp.* depicting class, order, and number of encoded DcaP proteins. **(B)** An unrooted tree of DcaP protein sequences from non-*Acinetobacter* species with AB5075 as the *A. baumannii* reference. Tree scale in amino acid substitutions.

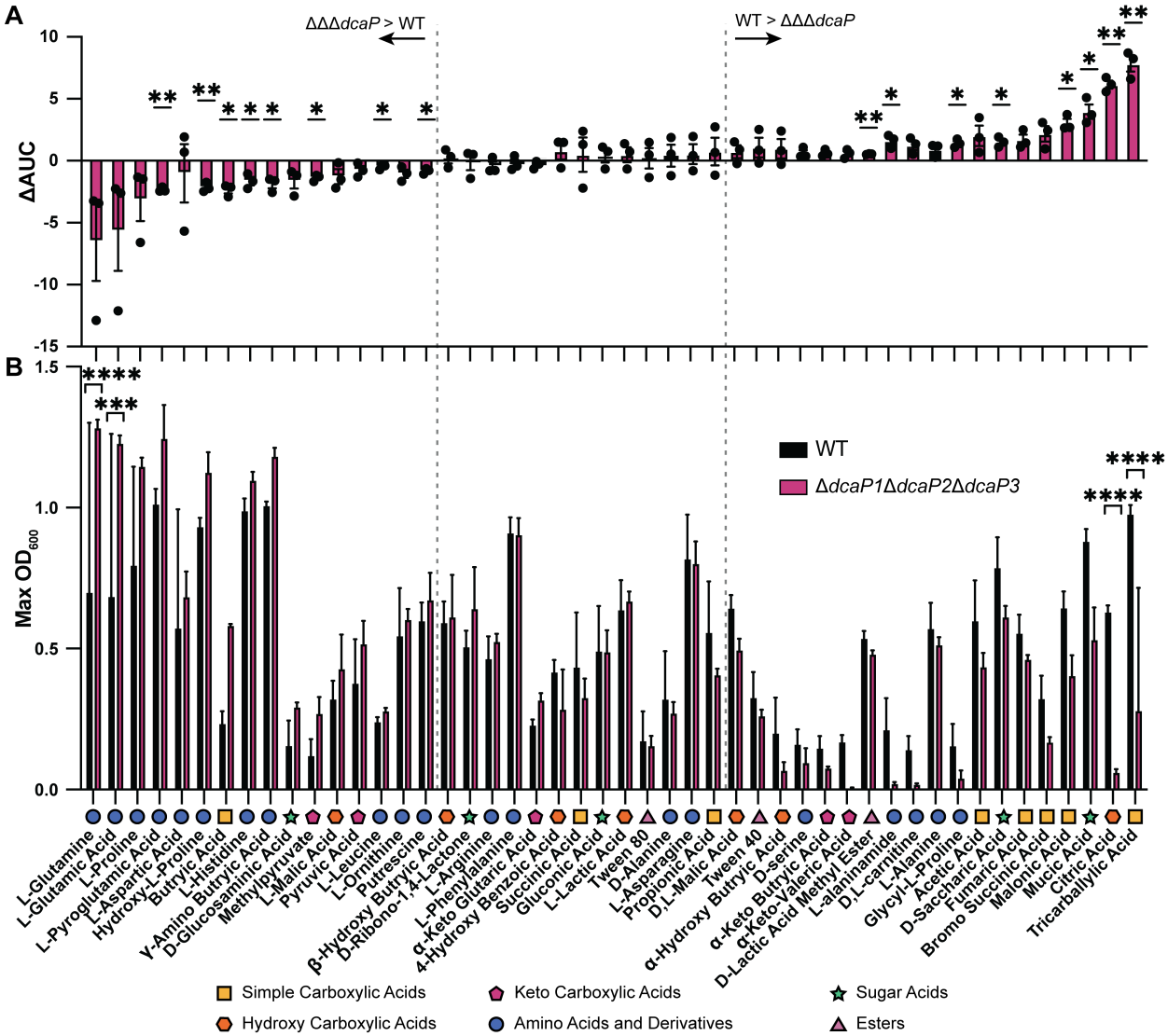

Figure 3. Wild-type *A. baumannii* grows better than ΔΔΔ*dcaP* mutant on certain di- and tricarboxylic acids as sole carbon sources. Biolog plates PM1 and PM2a were resuspended in M9 minimal media without a carbon source and inoculated with either WT or the ΔΔΔ*dcaP* mutant. (**A**) Difference in area under the curve (ΔAUC) was calculated for WT – ΔΔΔ*dcaP* mutant. Each point is from one experiment with 1 biological replicate per strain. Significance is by one sample t-test compared to 0. (**B**) Maximum optical density at 600 nm (OD_{600}) is shown. Significance is by two-way ANOVA with Sidak's multiple comparisons. Experiments were conducted three times with an n=1 for a total of n=3. Data are mean +/- SD. **P* < 0.05, ***P* < 0.01, ***P < 0.001, ****P < 0.0001

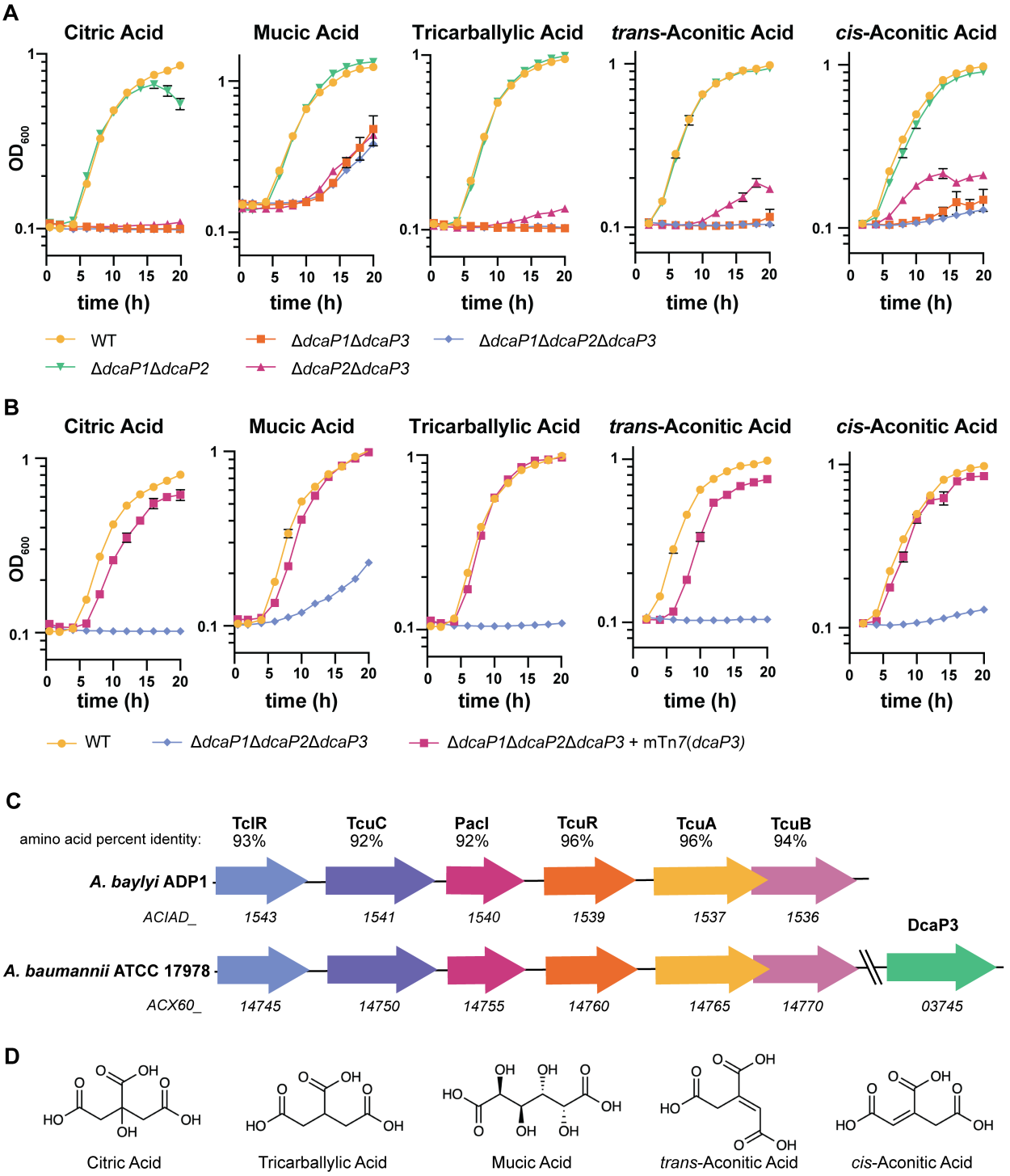

Figure 4. DcaP3 is important for growth on the carboxylic acid carbon sources citric acid, tricarballylic acid, mucic acid, and *cis*- and *trans*- aconitic acid. (A) Wildtype, double, and the triple ΔΔΔ*dcaP* mutants were grown in M9 media with the indicated compound as the sole carbon source. Optical density at 600 nm (OD_{600}) is shown. **(B)** Wildtype, the ΔΔΔ*dcaP* mutant, and the ΔΔΔ*dcaP* mutant complemented with *dcaP3* were grown on the indicated compound as the sole carbon source. **(C)** The genetic organization of the *tcu* metabolic locus and *dcaP3* in *A. baumannii* ATCC 17978. **(D)** The chemical structures of the relevant carbon source compounds. Data are mean +/- SEM and n=3. Experiments were repeated twice with similar results.

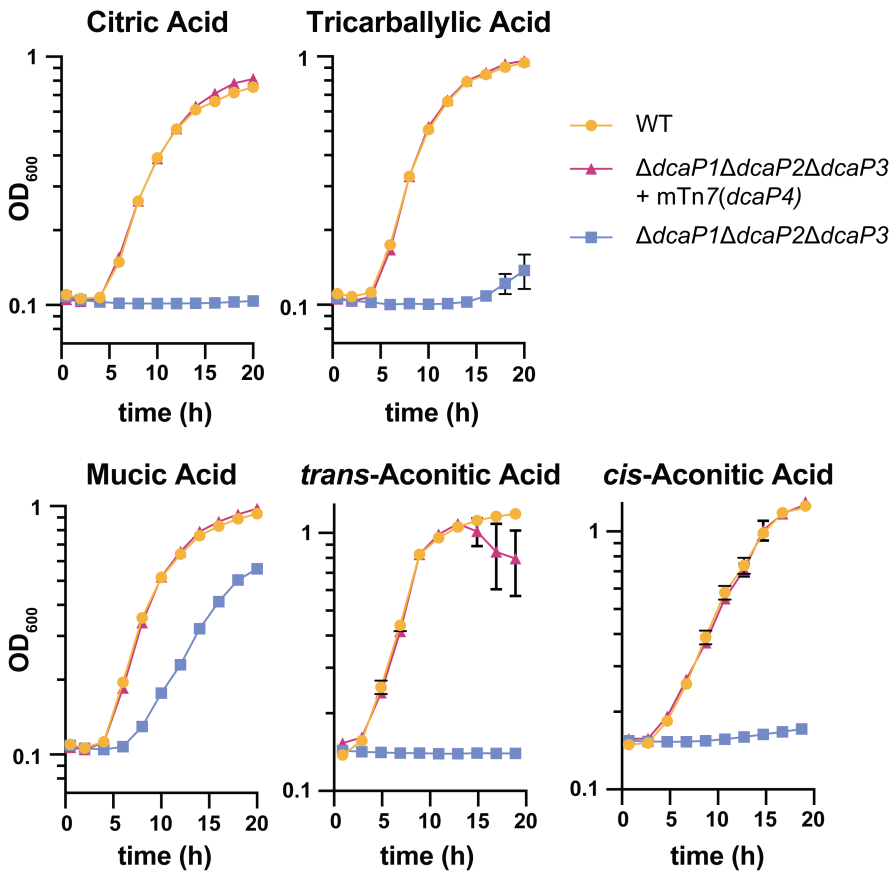

Figure 5. *A. baumannii* AB5075 DcaP4 complements growth of *A. baumannii* ATCC 17978 Δ*dcaP1-3* on citric acid, tricarballylic acid, mucic acid, and *cis*- and *trans*-aconitic acid. Wildtype, the ΔΔΔ*dcaP* mutant, and the ΔΔΔ*dcaP* mutant complemented with *dcaP4* were grown in M9 media with the indicated compound as the sole carbon source. Optical density at 600 nm (OD_{600}) is shown. Data are mean +/- SEM and n=3. Experiments were repeated twice with similar results.

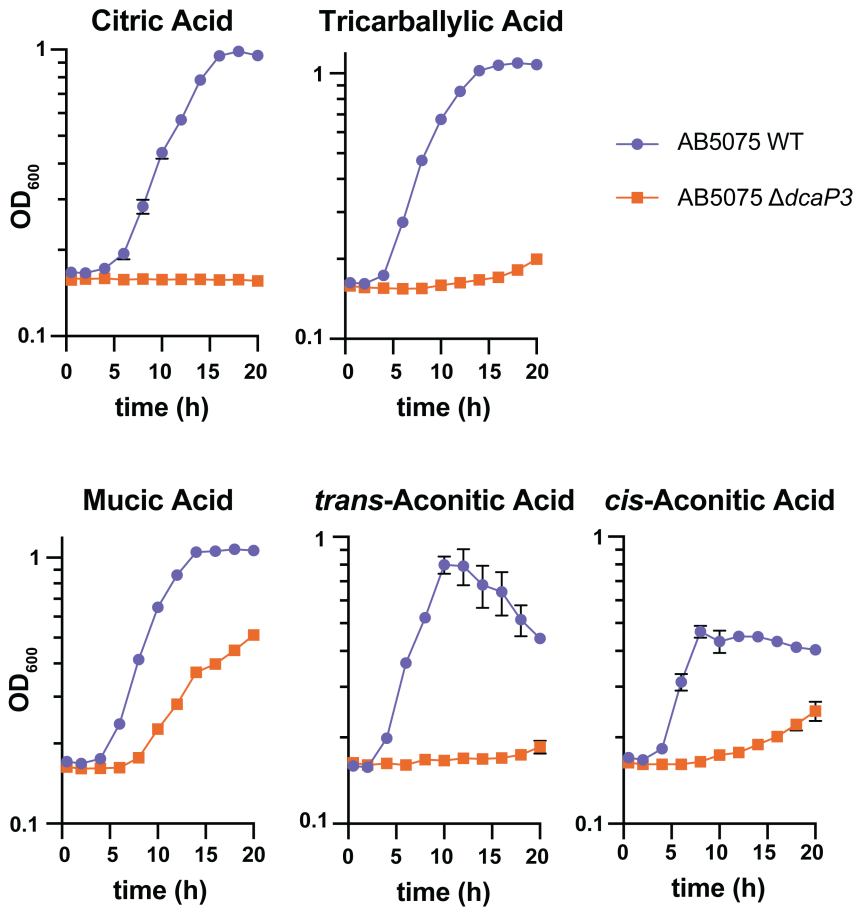

Figure 6. *A. baumannii* AB5075 Δ*dcaP3* is defective for growth on citric acid, tricarballylic acid, mucic acid, and *cis*- and *trans*-aconitic acid. *A. baumannii* AB5075 wild-type and Δ*dcaP3* mutant strains were grown in M9 media with the indicated compound as the sole carbon source. Optical density at 600 nm (OD_{600}) is shown. Data are mean +/- SEM and n=3. Experiments were repeated twice with similar results.

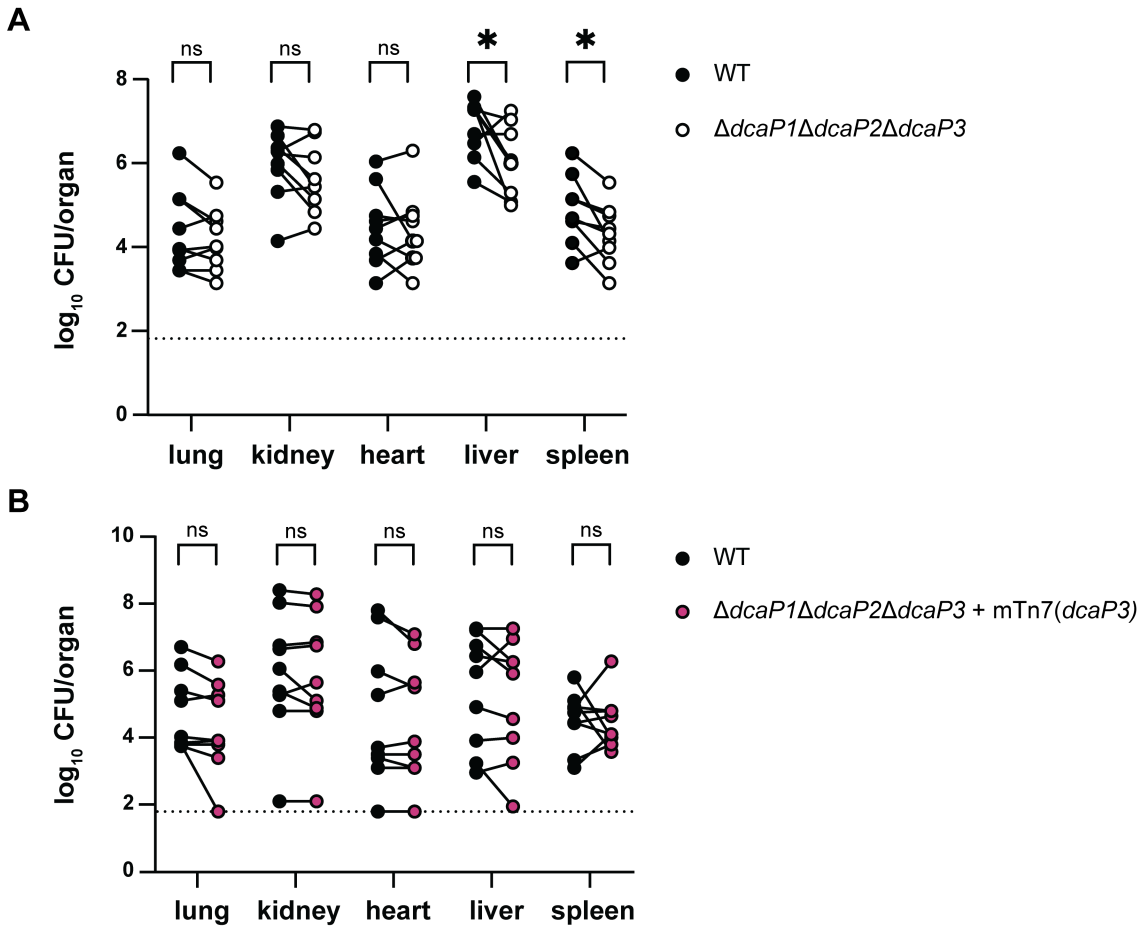

Figure 7. DcaP3 is important for infecting the liver and spleen in a model of bloodstream infection. (A-B) Wild-type and the indicated strains were retro-orbitally inoculated into Swiss Webster mice in a 1:1 ratio. At 24 h post-infection, organs were harvested and bacterial CFU were enumerated. The dotted lines indicate the limit of detection. Each point represents one strain enumerated from one mouse; n=9-10. Data are combined from two experiments. Statistics are Wilcoxon non-parametric test. *$P < 0.05$.